Extended Molecular Mechanics Simulation of Thermodynamic Quantities, Structures, and Vibrational Spectra of Fatty Acids

Isao YOKOYAMA, Yoshihisa MIWA, Katsunosuke MACHIDA,* Junzo UMEMURA,† and Soichi HAYASHI†
Faculty of Pharmaceutical Sciences, Kyoto University, Yoshida, Sakyo-ku, Kyoto, 606
† Institute for Chemical Research, Kyoto University, Uji, Kyoto-fu, 611
(Received September 28, 1992)

An extended molecular mechanics calculation of thermodynamic quantities, structure parameters, infrared absorption spectra, and Raman spectra of normal fatty acids was carried out on the basis of the potential and the intensity parameters transferred from those determined for acetic acid and normal paraffins in the gas phase. The overall features of the infrared absorption spectra of propionic acid and its deuterated species in the solid state at liquid-nitrogen temperature are successfully reproduced. The multiple CH_2 wagging bands of the cis-configuration of long-chain fatty acids are ascribed to the coupling between the C–O stretching mode and the $C_\alpha H_2$ or the $C_\beta H_2$ wagging mode. The infrared absorption spectra of lauric through palmitic acids at room temperature are well simulated by superimposing the spectra of the cis- and the trans-configurations. The simulated Raman spectrum of crystalline palmitic acid based on the bond polarizability model agrees well with the observed spectrum at room temperature.

An extended molecular mechanics simulation[1—3] of the thermodynamic quantities, the structures, and the vibrational spectra of monomers and dimers of formic and acetic acids has been carried out recently in our laboratory. The potential model including the effective nuclear charges and their fluxes,[4] which are used also as the infrared intensity parameters, elucidates well the changes in the geometries and the vibrational characteristics[5—14] of the carboxyl group on the dimerization simultaneously. The observed Raman spectra of formic acid and its deuterated species in the gas phase[8,9] were successfully reproduced on the basis of the bond polarizability model[15—17] including the bond polarizabilities and their derivatives with respect to certain internal coordinates. The variation in the half widths of the infrared absorption bands of formic and acetic acids in the solution in carbon tetrachloride and the Raman bands of acetic acid in the liquid state were simulated by introducing five half band width parameters[3] for the relevant internal coordinates.

Normal fatty acids in the solid state form centrosymmetric cyclic dimers in which the two carboxyl groups associate with each other by means of two equivalent hydrogen bonds. Previous infrared studies[18—21] revealed that the double proton transfer along the hydrogen bonds brings about the cis- and the trans-configurations as to the mutual orientation of the carbonyl and the alkyl groups (Fig. 1). Since the transferability of parameters is an essential requisite for the molecular mechanics calculation, it is desirable to test how far the potential and the intensity parameters[1—3] estimated from the experimental data of formic and acetic acids can be used for longer fatty acids. In this work, an extended molecular mechanics simulation for propionic through palmitic acids is carried out, and the calculated thermodynamic quantities and the structures of these fatty acids are compared with the observed data.[22—26] The infrared absorption and the Raman spectra of propionic acid in the liquid and the solid states, the infrared spectra of lauric, myristic, and palmitic acids in the solid state, and the Raman spectra of palmitic acid in the solid state are simulated in terms of the potential and the intensity parameters of the carboxyl group of acetic acid[3] and those of the alkyl group of alkanes.[27,28] The fitting is further improved by the revision of the potential and the intensity parameters related to the α- and the β-methylene groups of fatty acids (Tables 1, 2, and 3).

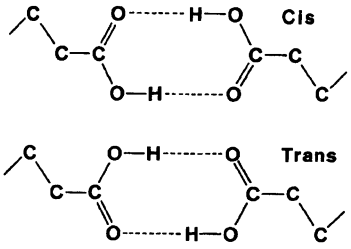

Fig. 1. Schematic representation of cis- and trans-configurations of fatty acid.

Calculation

Parametrization of the Model. The potential function is expressed in the following form:

$$V = \sum_l D_i \exp\{-a_i(r_i - r_i^0)\}[\exp\{-a_i(r_i - r_i^0)\} - 2] + (1/2)\sum_i\sum_j F_{ij}(R_i - R_i^0)(R_i - R_j^0) + (1/2)\sum_n\sum_i V_{ni}\{1 - (-1)^n \cos n\tau_{ni}\} + (1/2)\sum_i\sum_j V_{NB}(r_{ij}) + (1/2)\sum_i\sum_j q_i q_j(1/\varepsilon_{ij} r_{ij}). \quad (1)$$

The parameters in the first sum in Eq. 1 (the bond stretching Morse potential) were fixed at the values transferred from acetic acid,[3] except that the param-

Table 1. Potential Parameters

Bond stretching

r_i		a_i/Å^{-1}	D_i/aJ	r_i^0/Å	r_i	a_i/Å^{-1}	D_i/aJ	r_i^0/Å
H–O	(m)	2.1401*	0.7755*	1.000*	H–C_α	1.7974*	0.7278*	1.095*
	(d)	2.2010*	0.7927*	1.000*	H–C_β	1.8385	0.7308*	1.095*
C–O	(m)	2.2423*	0.6010*	1.330*	H–C	1.8196*	0.7308*	1.095*
	(d)	2.5410*	0.6010*	1.330*	C–C_α	2.1090*	0.5640*	1.500*
C=O	(m)	2.0840*	1.3500*	1.190*	C_α–C_β (CH_3CH_2)	1.9496	0.6045	1.520*
	(d)	2.0250	1.3500*	1.190*	C_α–C_β (CH_2CH_2)	1.9215	0.6223	1.520*
H···O	(d)	1.5500*	0.0480*	1.670*	C–C (CH_3CH_2)	1.9513*	0.5883*	1.520*
					C–C (CH_2CH_2)	1.9574*	0.5970*	1.520*

Intrinsic angles and general quadratic force constants (Diagonal)

θ_i		θ_i^0/deg	F_{ii}/aJ rad^{-2}	θ_i	θ_i^0/deg	F_{ii}/aJ rad^{-2}
C–O–H	(m)	102.5*	0.5515*	H–C_α–C	109.5*	0.6432*
	(d)	107.0*	0.7915*	H–C_α–C_β	109.5*	0.5800
O–C=O	(m)	126.0*	0.5200*	H–C_α–H	109.5*	0.5250
	(d)	126.0*	1.0500#	C–C_α–C_β	109.5*	0.6050
			1.2000##			
C_α–C–O	(m)	109.5*	0.8000*	H–C(H_2)–C	109.5*	0.5552*
	(d)	112.0*	0.9500#	H–C(H,C)–C	109.5*	0.5976[b]*
			0.7500##	C–C–C	109.5*	0.6779[b]*
C_α–C=O	(m)	124.5*	1.2226*	H–C–H (CH_3–)	109.5*	0.5146*
	(d)	122.0*	1.2226*	(–CH_2–)	109.5*	0.5206*
O–H···O						
(ipb)		0.0*	0.0050*			
(opb)		0.0*	0.1150*			
			0.1300##(cis)[a]			
			0.1350##(trans)[a]			
C=O···H		120.0*	0.0400*			
CO_2 opb		0.0*	0.3850*			

General quadratic force constants (Off-diagonal)[c]

Symbol	F_{ij}	Symbol	F_{ij}
Stretching-Stretching/N cm^{-1}		Bending-Bending/aJ rad^{-2}	
H–C_α, C_α–C	0.1191*	H–C_α–H, H–C_α–C	0.0352*
C_α–C, C–O	0.4344*	H–C_α–C, H–C_α–C	−0.0300*
C_α–C, C=O	0.0258*	C_α–C–O, C_α–C=O	−0.1637*
C–O, O–H	0.1271*	O–C=O, C_α–C=O	−0.1138*
O–C, C=O	0.4626*	C_α–C–O, C–O–H	−0.2200*
		H–O–C, O–C=O	−0.2450*
		H–C_α–C_β, H–C_α–C_β	−0.0500
Stretching-Bending/10^{-8} N rad^{-1}		H–C_α–C, H–C_α–C_β	−0.0250
H–C_α–C, H–C_α	0.5552*	H–C_α–C, C_α–C–O	0.1573C_τ[d]
H–C_α–C, C_α–C	0.2000	H–C_α–C, C_α–C=O	−0.2000C_τ
H–C_α–C_β, C_α–C	0.0400	C_β–C_α–C, C_α–C=O	0.1500$C_\tau^\#$
H–C_α–C_β, C_α–C_β	0.2147*	C_β–C_α–C, C_α–C–O	−0.3500$C_\tau^\#$
C_α–C=O, C_α–C	0.8092*	C_β–C_α–C, C_α–C=O	0.0500$C_\tau^{\#\#}$
C_α–C=O, C=O	−0.0286*	C_β–C_α–C, C_α–C–O	−0.1000$C_\tau^{\#\#}$
C_α–C–O, C–C_α	0.4008*		
C_α–C–O, C–O	0.4267*	Alkyl chain	
H–O–C, O–H	0.0728*	C–C, C–C; C common	0.1307*
H–O–C, C–O	−0.0104*	H–C–C, C–C; C–C common	0.2147*
O–C=O, C–O	0.4522*	C–C–C, C–C; C–C common	0.2653*
O–C=O, C=O	0.4856*	H–C–C, H–C–C; C–C common	−0.0126*
H–C_α–C, C–O	−0.1700##	H–C–C, C–C–C; C–C common	0.0135*
H–C_α–C_β, C–O	0.1700##	H–C–C, H–C–C; C–H common	0.0412*
H–C_β–C_α, C–O	−0.0850##	H–C–C, H–C–C	−0.1064C_τ*
H–C_β–C_γ, C–O	0.0850##	H–C–C, C–C–C	−0.1497C_τ*
		C–C–C, C–C–C	−0.2181C_τ*
		H–C–C′, H′–C′–C″	−0.0080[b]##

Table 1. (Continued)

Torsion potential parameters/10^{-2}aJ					
V_{3i}(H–C–C–H)		1.829×10^{-1}*	V_{2i}(O=C–O–H)	(m)	4.440*
V_{3i}(H–C–C–C)		1.329×10^{-1}*		(d)	2.100*
V_{3i}(C–C–C–C)		0.918×10^{-1}*	V_{2i}(C_α–C=O···H)		0.800*
V_{3i}(H–C_β–C_α–H)	(m)	0.900×10^{-1}	V_{2i}(O–C=O···H)		0.600*
	(d)	1.280×10^{-1}	V_{2i}(C_β–C_α–C–O)		-3.400×10^{-1}
V_{3i}(H–C_β–C_α–C)	(m)	0.660×10^{-1}	V_{2i}(C_β–C_α–C=O)		-3.400×10^{-1}
	(d)	0.930×10^{-1}	V_{3i}(C_β–C_α–C–O)		3.580×10^{-2}*
V_{3i}(H–C_α–C–O)		3.580×10^{-2}*	V_{3i}(C_β–C_α–C=O)		-3.580×10^{-2}*
V_{3i}(H–C_α–C=O)		-3.580×10^{-2}*	V_{6i}(C_β–C_α–C–O)	(m)	-0.400×10^{-1}
V_{2i}(C_α–C–O–H)	(m)	4.440*		(d)	-1.800×10^{-1}
	(d)	3.800*	V_{6i}(C_β–C_α–C=O)	(m)	-0.400×10^{-1}
				(d)	-1.800×10^{-1}

a) In order to fit the observed frequencies of the OH out-of-plane bending modes of crystalline longer fatty acids at liquid-nitrogen temperature, 963 cm^{-1} (cis) and 976 cm^{-1} (trans), these force constants were distinguished. b) In case of long-chain fatty acid dimers in the C-form crystal, slight modification of F(HCC) (from 0.5976 to 0.5800) and introduction of F (H–C–C′, H′–C′–C″) were necessary for adjusting the observed frequencies of the methylene wagging modes. It was favorable to reduce F (CCC) to 0.600 for reproducing the observed frequencies of the CCC bending modes of the dimers in the crystal. c) The off-diagonal force constants of the carboxyl group of the monomers omitted in this table were transferred from those used for acetic acid monomer (Ref. 3). d) The dependence on the dihedral angle A–B–C–D is introduced by using a factor $C_\tau = \cos \tau_{A-B-C-D}$. The symbol * denotes the transferred value from acetic acid or alkane. The symbols # and ## indicate the parameters used for propionic acid and long-chain fatty acids, respectively. Abbreviation; m: monomer, d: dimer, ipb: in-plane bending, opb: out-of-plane bending.

Table 2. Bond Charge Parameters and Bond Charge Fluxes for Fatty Acids

Bond charge parameters			Angle bending fluxes[b]/e rad^{-1}			
Heterogeneous β/e[a]			CO_2 group		COH group	
O–H	(m)	0.2390*	$\partial q_{C=O}/\partial\theta_{O-C=O}$	0.130*	$\partial q_{OH}/\partial\theta_{COH}$	0.050*
	(d)	0.1300*	$\partial q_{C=O}/\partial\theta_{C_\alpha-C=O}$	−0.100*	$\partial q_{O-C}/\partial\theta_{COH}$	0.050*
C–O		0.0193*	$\partial q_{C=O}/\partial\theta'_{C_\alpha-C-O}$	−0.030*		
C=O		0.3187*	$\partial q_{C-O}/\partial\theta_{O-C=O}$	0.130*		
H–C_α		0.1500*	$\partial q_{C-O}/\partial\theta'_{C_\alpha-C=O}$	−0.065*		
H–C(–CH_2–)		0.1250*	$\partial q_{C-O}/\partial\theta_{C_\alpha-C-O}$	−0.065*		
H–C(CH_3–)		0.1000*				
Homogeneous γ/e[a]					$C–C_\alpha H_2–C_\beta$ group	
C–C_α		0.1380*	$\partial q_{C_\alpha H}/\partial\theta_{HC_\alpha C}$	−0.015*	$\partial q_{C_\alpha H}/\partial\theta'_{CC_\alpha C_\beta}$	0.0025
C_α–C_β		0.0480	$\partial q_{C_\alpha H}/\partial\theta_{HC_\alpha H}$	−0.005*	$\partial q_{C_\alpha H}/\partial\theta'_{HC_\alpha C}$	0.020*
			$\partial q_{C_\alpha C_\beta}/\partial\theta_{HC_\alpha C_\beta}$	0.008*	$\partial q_{C_\alpha H}/\partial\theta'_{HC_\alpha C_\beta}$	−0.0025
Bond stretching fluxes[b]/e Å^{-1}			$\partial q_{C_\alpha C_\beta}/\partial\theta'_{HC_\alpha C}$	−0.009*	$\partial q_{C_\alpha C}/\partial\theta_{HC_\alpha C}$	−0.004*
$\partial q_{OH}/\partial r_{HO}$	(m)	−0.110*	$\partial q_{C_\alpha C_\beta}/\partial\theta'_{HC_\alpha H}$	0.002*	$\partial q_{C_\alpha C}/\partial\theta'_{HC_\alpha C_\beta}$	0.002
	(d)	0.780*			$\partial q_{C_\alpha C}/\partial\theta'_{HC_\alpha H}$	0.004*
$\partial q_{O-C}/\partial r_{C-O}$	(m)	0.760*				
	(d)	1.138*			CH_3 group	
$\partial q_{O=C}/\partial r_{C=O}$	(m)	0.680*	$\partial q_{CH}/\partial\theta_{HCH}$	−0.003*	$\partial q_{CC}/\partial\theta'_{HCH}$	−0.003*
	(d)	0.550*	$\partial q_{CH}/\partial\theta_{HCC}$	−0.002*	$\partial q_{CC}/\partial\theta_{HCC}$	0.003*
$\partial q_{O\cdots H}/\partial r'_{C=O}$	(d)	0.240*	$\partial q_{CH}/\partial\theta'_{HCH}$	0.006*		
$\partial q_{CC_\alpha}/\partial r_{CC_\alpha}$		−0.020*	$\partial q_{CH}/\partial\theta'_{HCC}$	0.001*		
$\partial q_{C_\alpha H}/\partial r_{HC_\alpha}$		−0.100*				
$\partial q_{C_\beta H}/\partial r_{HC_\beta}$		−0.100*			CH_2 group	
$\partial q_{CH}/\partial r_{HC}$		−0.216*	$\partial q_{CH}/\partial\theta_{HCH}$	−0.005*	$\partial q_{CC}/\partial\theta_{HCC}$	0.008*
$\partial q_{CH}/\partial r'_{HC}$		−0.035*	$\partial q_{CH}/\partial\theta'_{HCC}$	−0.0025*	$\partial q_{CC}/\partial\theta'_{HCH}$	0.002*
$\partial q_{CH}/\partial r'_{CC}$ (CH_3C)		−0.030*	$\partial q_{CH}/\partial\theta'_{CCC}$	0.010*	$\partial q_{CC}/\partial\theta'_{HCC}$	−0.009*

a) e=electronic unit. b) The meaning of the symbols is the same as those reported previously (Refs. 1—3). The symbol * denotes the transferred value from acetic acid or alkane. Abbreviation; m: monomer, d: dimer.

Table 3. Bond Polarizability Parameters and their Derivatives for Fatty Acids

Equilibrium parameters[a]/Å^3 [b]							
γ^L_{OH}	0.100*	α^E_{OH}	0.500*	$\gamma^L_{C_\alpha H}$	0.290*	$\alpha^E_{C_\alpha H}$	0.545*
γ^L_{C-O}	1.050*	α^E_{C-O}	0.540*	$\gamma^L_{CH}(CH_3)$	0.300[c]*	α^E_{CH}	0.530[c]*
$\gamma^L_{C=O}$	0.810*	$\alpha^E_{C=O}$	0.800*	(CH_2)	0.350[c,d]*		
$\gamma^L_{CC_\alpha}$	1.230*	$\alpha^E_{CC_\alpha}$	0.265*	γ^L_{CC}	1.050[c]*	α^E_{CC}	0.240*
$\gamma^L_{C_\alpha C_\beta}$	1.070*	$\alpha^E_{C_\alpha C_\beta}$	0.240*	$\gamma^T_{CH,C}$	0.075*		
Derivatives for stretching coordinates[a]/Å^2 [b]							
$\partial\gamma^L_{C-O}/\partial r_{C-O}$		0.400*		$\partial\alpha^E_{C-O}/\partial r_{C-O}$		0.300*	
$\partial\gamma^L_{C=O}/\partial r_{C=O}$		2.820*		$\partial\alpha^E_{C=O}/\partial r_{C=O}$		0.940*	
$\partial\gamma^L_{CC_\alpha}/\partial r_{CC_\alpha}$		0.900*		$\partial\alpha^E_{CC_\alpha}/\partial r_{CC_\alpha}$		1.000*	
$\partial\gamma^L_{C_\alpha C_\beta}/\partial r_{C_\alpha C_\beta}$		1.400*		$\partial\alpha^E_{C_\alpha C_\beta}/\partial r_{C_\alpha C_\beta}$		0.500*	
$\partial\gamma^L_{CC}/\partial r_{CC}$ (CH_3CH_2)		1.400*		$\partial\alpha^E_{CC}/\partial r_{CC}$ (CH_3CH_2)		0.500*	
$\partial\gamma^L_{CC}/\partial r_{CC}$ (CH_2CH_2)		1.900[c]*		$\partial\alpha^E_{CC}/\partial r_{CC}$ (CH_2CH_2)		0.400[c]*	
$\partial\gamma^L_{CH}/\partial r_{CH}$		1.980*		$\partial\alpha^E_{CH}/\partial r_{CH}$		0.450*	
Derivatives for bending coordinates/Å^3 rad^{-1} [b]							
CO_2 group				COH group			
$\partial\gamma^L_{C=O}/\partial\theta_{OC=O}$		−0.350*		$\partial\gamma^L_{HO}/\partial\theta_{COH}$		0.200*	
$\partial\gamma^L_{C=O}/\partial\theta_{C_\alpha C=O}$		0.100*		$\partial\alpha^E_{HO}/\partial\theta_{COH}$		0.095*	
$\partial\gamma^L_{C=O}/\partial\theta'_{C_\alpha C-O}$		0.250*					
C-$C_\alpha H_2$-C_β group							
$\partial\gamma^L_{C-O}/\partial\theta'_{HC_\alpha H}$		−0.430		$\partial\alpha^E_{C-O}/\partial\theta'_{HC_\alpha H}$		−0.220	
$\partial\gamma^L_{HC_\alpha}/\partial\theta_{HC_\alpha C}$		−0.030*		$\partial\alpha^E_{HC_\alpha}/\partial\theta_{HC_\alpha C}$		0.300*	
$\partial\gamma^L_{HC_\alpha}/\partial\theta_{HC_\alpha H}$		−0.135*		$\partial\alpha^E_{HC_\alpha}/\partial\theta_{HC_\alpha C_\beta}$		0.300*	
$\partial\gamma^L_{HC_\alpha}/\partial\theta_{HC_\alpha C_\beta}$		−0.050*		$\partial\alpha^E_{HC_\alpha}/\partial\theta'_{HC_\alpha C}$		−0.300*	
$\partial\gamma^L_{HC_\alpha}/\partial\theta'_{CC_\alpha C_\beta}$		0.1275		$\partial\alpha^E_{HC_\alpha}/\partial\theta'_{HC_\alpha C_\beta}$		−0.300*	
$\partial\gamma^L_{HC_\alpha}/\partial\theta'_{HC_\alpha C}$		0.050*		$\partial\alpha^E_{CC_\alpha}/\partial\theta_{CC_\alpha C_\beta}$		−0.070	
$\partial\gamma^L_{HC_\alpha}/\partial\theta'_{HC_\alpha C_\beta}$		0.0375		$\partial\alpha^E_{CC_\alpha}/\partial\theta_{HC_\alpha C}$		0.070*	
$\partial\gamma^L_{CC_\alpha}/\partial\theta_{CC_\alpha C_\beta}$		−0.130		$\partial\alpha^E_{CC_\alpha}/\partial\theta'_{HC_\alpha H}$		−0.070*	
$\partial\gamma^L_{CC_\alpha}/\partial\theta_{HC_\alpha C}$		0.050*		$\partial\alpha^E_{C_\beta C_\alpha}/\partial\theta_{CC_\alpha C_\beta}$		0.100*	
$\partial\gamma^L_{CC_\alpha}/\partial\theta'_{HC_\alpha C_\beta}$		0.040		$\partial\alpha^E_{C_\beta C_\alpha}/\partial\theta_{HC_\alpha C_\beta}$		−0.035*	
$\partial\gamma^L_{CC_\alpha}/\partial\theta'_{HC_\alpha H}$		−0.050*		$\partial\alpha^E_{C_\beta C_\alpha}/\partial\theta'_{HC_\alpha H}$		−0.030*	
$\partial\gamma^L_{C_\beta C_\alpha}/\partial\theta_{CC_\alpha C_\beta}$		−0.130*		$\partial\gamma^L_{C_\beta C_\alpha}/\partial\theta'_{HC_\alpha C}$		0.085*	
$\partial\gamma^L_{C_\beta C_\alpha}/\partial\theta_{HC_\alpha C_\beta}$		−0.055*		$\partial\gamma^L_{C_\beta C_\alpha}/\partial\theta'_{HC_\alpha H}$		0.070*	
CH_2 group[c]						CH_3 group	
$\partial\gamma^L_{HC}/\partial\theta_{HCC}$	−0.060*	$\partial\alpha^E_{HC}/\partial\theta_{HCC}$	0.260*			$\partial\gamma^L_{HC}/\partial\theta_{HCC}$	−0.100*
$\partial\gamma^L_{HC}/\partial\theta_{HCH}$	−0.260*	$\partial\alpha^E_{HC}/\partial\theta'_{CCC}$	0.080*			$\partial\gamma^L_{HC}/\partial\theta_{HCH}$	−0.200*
$\partial\gamma^L_{HC}/\partial\theta'_{CCC}$	0.125*	$\partial\alpha^E_{HC}/\partial\theta'_{HCC}$	−0.300*			$\partial\gamma^L_{HC}/\partial\theta'_{HCC}$	0.150*
$\partial\gamma^L_{HC}/\partial\theta'_{HCC}$	0.1275*	$\partial\alpha^E_{CC}/\partial\theta_{CCC}$	0.130*			$\partial\gamma^L_{HC}/\partial\theta'_{HCH}$	0.200*
$\partial\gamma^L_{CC}/\partial\theta_{CCC}$	−0.130*	$\partial\alpha^E_{CC}/\partial\theta_{HCC}$	−0.040*			$\partial\gamma^L_{CC}/\partial\theta^i_{HCC}$	0.200*
$\partial\gamma^L_{CC}/\partial\theta_{HCC}$	−0.080*	$\partial\alpha^E_{CC}/\partial\theta'_{HCH}$	−0.050*			$\partial\gamma^L_{CC}/\partial\theta^0_{HCC}$	−0.100*
$\partial\gamma^L_{CC}/\partial\theta'_{HCC}$	0.030*					$\partial\alpha^E_{CC}/\partial\theta^i_{HCC}$	0.120*
$\partial\gamma^L_{CC}/\partial\theta'_{HCH}$	0.200*					$\partial\alpha^E_{CC}/\partial\theta^0_{HCC}$	−0.060*

a) These parameters are used for carboxylic acid dimer. b) 1Å$=10^{-10}$ m. 1Å$^3\simeq1.11265\times10^{-40}$ C m^2 V^{-1}. c) The parameters were modified from those in Ref.27 (Machida et al.) for the purpose of fitting the observed Raman spectra of the longer normal paraffins. d) In case of the C_β–H bond of the β-methylene group, $\gamma^L_{C_\beta H}$ is 0.400. The symbol * denotes the transferred value from acetic acid or alkane.

eter a_i of the C=O bond was so reduced as to fit the bserved C=O stretching frequencies of fatty acids in the crystal.[19,20] Slight modification of the parameters D_i and a_i of the $C_\alpha H_2$–$C_\beta H_3$ and the $C_\alpha H_2$–$C_\beta H_2$ bonds taken from alkanes[28] was found necessary for reproducing the heats of formation[26] of propionic through nonanoic acids and the infrared absorption frequency of propionic acid contributed by the C_α–C_β stretching mode.[20]

In the general valence-type quadratic potential (the second sum in Eq. 1), the force constants concerning the carboxyl group and the α-methylene group were transferred from acetic acid,[3] while those concerning the alkyl chain were transferred from alkanes.[28] The force constants related to the α-methylene group were then adjusted by referring to the observed frequencies and the infrared absorption intensities of propionic acid dimer and its deuterated homologue.[20] All the intrinsic values of the bond lengths and the valence angles were fixed at the values taken from acetic acid[3] and

Table 4. Experimental and Calculated Geometries for Propionic Acid Monomer and Dimer

	Monomer				Dimer		
	Exptl		Calcd		Exptl		Calcd
Geometry[a]	Gas[b]	Gas[c]	MM3[d]	This work	Gas[b]	Cryst[e]	This work
r(O–H)/Å	0.97	0.970	—	0.998	1.03	—	1.056
r(C–O)/Å	1.367	1.352	1.366	1.348	1.329	1.324	1.330
r(C=O)/Å	1.211	1.210	1.213	1.209	1.232	1.226	1.230
r(C–C_α)/Å	1.518	1.509	1.496	1.508	1.518	1.502	1.512
r(C_α–C_β)/Å	1.543	1.523	1.528	1.538	1.547	1.536	1.538
r(O···O)/Å[f]	2.257	2.245	—	2.247	2.259	—	2.265
r(O···O)/Å[g]	—	—	—	—	2.711	2.644	2.703
∠(C–O–H)/°	107.0	105.8	—	106.7	110.0	—	109.7
∠(O–C=O)/°	122.1	—	121.6	123.0	123.7	122.2	124.4
∠(C_α–C–O)/°	111.2	111.8	111.8	110.7	113.4	113.7	112.1
∠(C_α–C=O)/°	126.7	125.8	126.6	126.3	122.9	124.0	123.5
∠(C–C_α–C_β)/°	112.8	112.7	113.0	112.7	112.0	113.0	113.5

a) 1Å=10^{-10} m. b) Electron diffraction data (Derrisen, Ref. 22). c) Microwave data (Stiefvater, Ref. 23). d) Allinger et al., Ref. 31. e) X-Ray diffraction data (Strieter et al., Ref. 24). f) Intramolecular distance between the oxygen of the hydroxyl group and that of the carbonyl group. g) Hydrogen-bonded distance in the dimer.

Table 5. Experimental and Calculated Geometries for Butyric Acid Dimer

Geometry[a]	Exptl[b]	Calcd	Geometry	Exptl[b]	Calcd
r(C–O)/Å	1.32	1.326	∠(O–C=O)/°	123	124.3
r(C=O)/Å	1.20	1.230	∠(C_α–C–O)/°	113	112.5
r(C–C_α)/Å	1.52	1.514	∠(C_α–C=O)/°	124	123.2
r(C_α–C_β)/Å	1.51	1.540	∠(C–C_α–C_β)/°	114	113.0
r(C_β–C_γ)/Å	1.52	1.538	∠(C_α–C_β–C_γ)°	111	111.3
r(O···O)/Å[c]	—	2.260			
r(O···O)/Å[d]	2.62	2.703			

a) 1Å=10^{-10} m. b) X-Ray diffraction data (Strieter and Templeton, Ref. 25). c) Intramolecular distance between the oxygen of the hydroxyl group and that of the carbonyl group. d) Hydrogen-bonded distance in the dimer.

alkanes.[28] The cross term between the H–C_α–C and the C_α–C–O bending coordinates, F_{ij}(H–C_α–C, C_α–C–O), and that between the H–C_α–C and the C_α–C=O bending coordinates, F_{ij}(H–C_α–C, C_α–C=O), were so modified as to reproduce the splitting of the bands due to the C–O stretching modes between the cis- and the trans-configurations.[20] The quadratic diagonal force constants, F(O–C=O) and F(C_α–C–O), and the off-diagonal constants, F_{ij}(C–C_α–C_β, C_α–C–O) and F_{ij}(C–C_α–C_β, C_α–C=O), were adjusted by referring to the observed frequencies of the O–C=O bending and the CO_2 rocking modes of propionic acid dimer in the crystal.[20]

In the third sum in Eq. 1, the torsional parameters used for the carboxyl group of acetic acid[3] were transferred to longer fatty acids. The potential barriers for the dihedral angles C_β–C_α–C–O and C_β– C_α–C=O were newly estimated in the following way. The three-fold torsional parameters V_3 for these two angles were transferred from the H–C_α–C–O and the H–C_α–C=O torsions of acetic acid.[3] The two-fold and six-fold torsional parameters, V_2 and V_6, were then fitted to the A_u and the B_g observed frequencies,[20] 121 and 94 cm^{-1}, of the C–C_α torsion modes of propionic acid dimer in the crystal. Concerning the above torsional parameters of propionic acid monomer, reduction of V_6 of the dimer was found necessary for fitting the observed frequency[23] (64 cm^{-1}) of the C–C_α torsion mode in the gas phase. The three-fold torsional parameters V_3 for the two dihedral angles H–C_β–C_α–C and H–C_β–C_α–H of propionic acid monomer were estimated by scaling the relevant torsional parameters of alkane[28] by a factor of 0.5. As a result, the calculated rotational barrier of the C_α–C_β bond (9.70 kJ mol^{-1}) and the frequency of the C_α–C_β torsion (201 cm^{-1}) agree well with the observed values in the gas phase, 9.79 kJ mol^{-1} and 190 cm^{-1},[23] respectively. The above two torsional parameters of the dimer, V_3 (H–C_β–C_α–C) and V_3 (H–C_β–C_α–H), must be reduced by a factor of 0.7 in order to reproduce the A_u and the B_g observed frequencies of the C_α–C_β torsion of propionic acid dimer in the crystal, 226 and 236 cm^{-1}.[20] The potential parameters in the first through the third sums of Eq. 1 are summarized in Table 1.

The nonbonded atom-atom potential parameters in the fourth sum in Eq. 1 were fixed to the values used for formic and acetic acids.[1—3] In the last sum representing the Coulomb potential, the effective atomic charges, q_i, are approximated as linear functions of internal coordinates. The atomic charge fluxes[1—3,28] (the sum of $\partial q_{ki}/\partial R_p$ with respect to the atom k) and the effective atomic charges[29] at the optimized geometry are used commonly as the infrared absorption intensity parameters and the Coulomb potential parameters. The intrinsic atomic charges were calculated from the Pauling electronegativities,[30] χ_i, and the bond charge

Table 6. Experimental and Calculated Heats of Formation and Entropies of Fatty Acid Monomers

Compound	ΔH_f/kJ mol^{-1}			S/J mol^{-1}deg^{-1}	
	Exptl[a]	Calcd		Exptl	Calcd
		MM3[b]	This work		This work
Formic acid	−378.7±0.6	−377.6	−378.8[c]	249[d]	248[c]
Acetic acid	−432.8±1.5	−431.9	−432.3[e]	283[d]	286[e]
Propionic acid	−453.5±0.5	−452.2	−453.3	—	316
Butyric acid	−475.8±4.1	−472.6	−474.0	—	347
Pentanoic acid	−491.9±3.0	−493.2	−493.4	—	378
Hexanoic acid	−511.9±2.3	−513.7	−513.8	—	409
Heptanoic acid	−536.2±2.1	−534.3	−534.4	—	440
Octanoic acid	−554.3±1.5	−554.9	−555.0	—	472
Nonanoic acid	−577.3±2.1	—	−575.6	—	503

a) Pedley et al., Ref. 26. b) Allinger et al., Ref. 31. c) Yokoyama et al., Ref. 1. d) Stull et al., Ref. 34. e) Yokoyama et al., Ref. 3.

Table 7. Half Band Width Parameters for Fatty Acids

Internal coordinate		η_i[a]	
		Liquid and Solution (CCl_4)	Crystal
OH	Stretching (dimer)	*70.0	*70.0
COH	Bending	*6.0	1.0
OH···O	Out-of-plane bending	*8.0	*8.0[b]
$HC_\alpha C$, $HC_\alpha C_\beta$	Bending	*2.0	1.0
$HC_\alpha H$	Bending (α-methylene)	6.0[c] (Raman)	1.0
$C_\alpha C$–O, $C_\alpha C$=O	Bending	5.0	1.0
C=O	Stretching	*1.0	10.0[d] (Raman)
HCH	Bending (alkyl group)	*1.0	2.0[d] (Raman)

a) The half band width parameter for the internal coordinate not listed in Table 7 is 1.0. b) The half band width parameter for the OH out-of-plane bending in the crystalline state was used only for spectral simulation at room temperature. c) The value used for infrared spectra in CCl_4 solution is 1.0. d) This value is used only for Raman spectra. The symbol * denotes the transferred value from acetic acid (Ref. 3).

Table 8. Experimental and Calculated Vibrational Frequencies of the O–C=O Bending Modes and the CO_2 Rocking Modes of Propionic Acid through Palmitic Acid

Compound		Freq/cm^{-1}							
		δ O–C=O				ρ CO_2			
		Cis		Trans		Cis		Trans	
		Exptl	Calcd	Exptl	Calcd	Exptl	Calcd	Exptl	Calcd
Propionic acid	B_u	654[a]	654	(640)[a,b]	646	512[a]	508	(560)[a,b]	545
	A_g	644[a]	644	(627)[a,b]	638	483[a]	492	(541)[a,b]	525
Octanoic acid	B_u	691[c]	693	672,670[c]	674		545		557
Decanoic acid	B_u	694[c]	694	678,670[c]	674	547[c]	545	567[c]	559
Lauric acid	B_u	695[c]	694	678,668[c]	674		552		565
Myristic acid	B_u	693[c]	694	674[c]	674		557		566
Palmitic acid	B_u	695[c]	694	679,671[c]	674		557		566

a) Umemura, Ref. 20. b) Calculated value. c) Hayashi and Umemura, Ref. 19. Abbreviation; δ: bending, ρ: rocking.

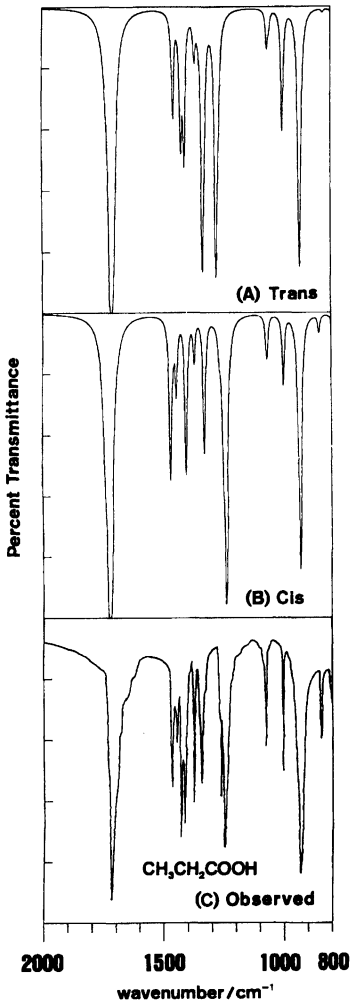

Fig. 2. Infrared spectra of crystalline propionic acid at 113 K. (A) Simulated ($\omega_0=10$ cm^{-1}); trans-configuration, (B) Simulated ($\omega_0=10$ cm^{-1}); cis-configuration, (C) Observed, reproduced from *Bull Inst. Chem. Res., Kyoto Univ.*, **46**, 213 (1968) (Ref. 18) with permission of Institute for Chemical Research, Kyoto University. The bands due to the Fermi resonance (above 1500 cm^{-1}) in the observed spectra were eliminated.

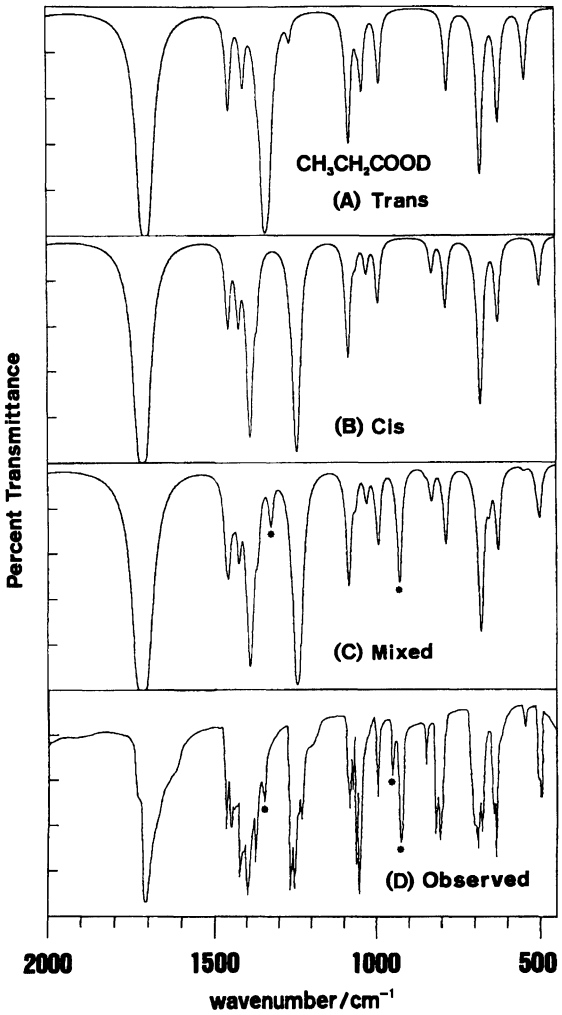

Fig. 3. Infrared spectra of crystalline carboxyl-deuterated propionic acid at liquid-nitrogen temperature (Simulation, $\omega_0=15$ cm^{-1}). (A) Simulated; *trans*-CH_3CH_2COOD, (B) Simulated; *cis*-CH_3CH_2COOD, (C) Simulated; *cis*-CH_3CH_2COOD + *cis*-CH_3CH_2COOH (1:0.3), (D) Observed, reproduced from *J. Mol. Struct.*, **36**, 35 (1977) (Ref. 20) with permission of Elsevier Science Publishers B. V. The bands due to the Fermi resonance (above 1500 cm^{-1}) in the observed spectra were eliminated.

parameters, β_{ki} and γ_{li},[3] according to Eq. 2;

$$q_i^0 = \sum_k \beta_{ki}(\chi_k - \chi_i) + \sum_l \gamma_{li}. \quad (2)$$

The heterogeneous bond charge parameter β_{ki} expresses the charge flow from the atom k to the atom i on the formation of the bond ki between two atoms of different elements, while the homogeneous parameter γ_{li} is used for the bond formed between two atoms of the same element. The homogeneous bond charge parameter γ_{li} for the C–C_α bond, 0.138 e, was estimated from the experimental dipole moment and its direction of acetic acid monomer.[3] Addition of a single parameter γ_{li} for the C_α–C_β bond, 0.048 e, proved to reproduce both the magnitude and the direction of the experimental dipole moment of propionic acid monomer[23] on fixing the other bond charge parameters at the values transferred from acetic acid[3] and alkanes.[28] All the charge fluxes on the bond stretching and the angle bending of the carboxyl group of acetic acid were transferred to longer fatty acids. The bond charge flux of the H–C_β bond was taken to be the same as that of the H–C_α bond of acetic acid.[3] This parameter is consistent with the weak infrared absorption intensities of the H–C_β stretching modes of propionic acid in the carbon tetrachloride solution. The angle bending fluxes concerning the α-methylene group were estimated in the following way. The values transferred from the α-methyl group of acetic acid[3] were combined with those of the methylene group of alkane,[28] and were given the minimum

Table 9. Atomic Net Charges of cis- and trans-Configurations of Propionic Acid Dimer and Lauric Acid Dimer

Charge/e[a)]	H(–O)	O(–C)	C(=O)	O(=C)	C_α	H ($-C_\alpha$)	C_β	H($-C_\beta$)
Propionic acid dimer								
cis	0.251	−0.270	0.270	−0.389	−0.031	0.060	−0.067[b)]	0.039[b)]
trans	0.252	−0.278	0.280	−0.392	−0.031	0.060	−0.067[b)]	0.038[b)]
Lauric acid dimer								
cis	0.250	−0.266	0.267	−0.389	−0.031	0.060	−0.050[b)]	0.049[b)]
trans	0.251	−0.271	0.270	−0.387	−0.031	0.060	−0.050[b)]	0.049[b)]

a) electronic unit. b) propionic acid; $C_\beta H_3$ group, lauric acid; $C_\beta H_2$ group.

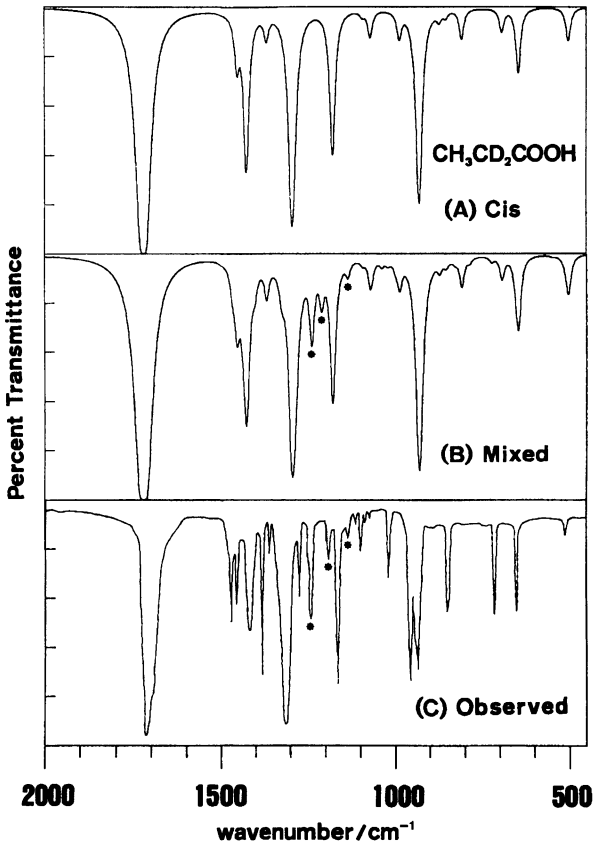

Fig. 4. Infrared spectra of crystalline α-methylene-deuterated propionic acid at liquid-nitrogen temperature (Simulation, ω_0=15 cm^{-1}). (A) Simulated; *cis*-CH_3CD_2COOH, (B) Simulated; CH_3CD_2COOH+$CH_3CHDCOOH$+CH_3CH_2COOH (1:0.2:0.15), (C) Observed, reproduced from *J. Mol. Struct.*, **36**, 35 (1977) (Ref. 20) with permission of Elsevier Science Publishers B. V. The bands due to the Fermi resonance (above 1500 cm^{-1}) in the observed spectra were eliminated.

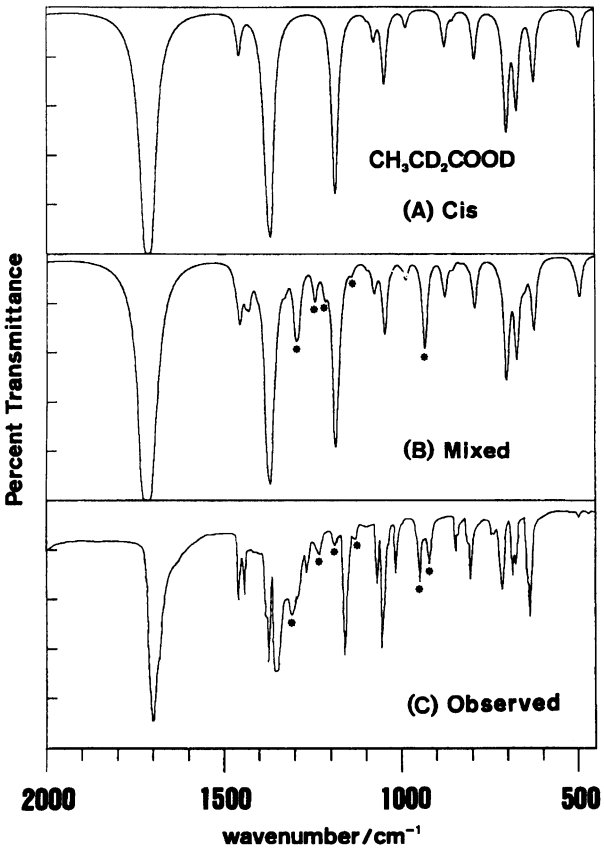

Fig. 5. Infrared spectra of crystalline α-methylene- and carboxyl-deuterated propionic acid at liquid-nitrogen temperature (Simulation, ω_0=15 cm^{-1}). (A) Simulated; *cis*- CH_3CD_2COOD, (B) Simulated; CH_3CD_2COOD+$CH_3CHDCOOH$+CH_3CD_2COOH +CH_3CH_2COOH (1: 0.1:0.1:0.05), (C) Observed, reproduced from *J. Mol. Struct.*, **36**, 35 (1977) (Ref. 20) with permission of Elsevier Science Publishers B. V. The bands due to the Fermi resonance (above 1500 cm^{-1}) in the observed spectra were eliminated.

revision to satisfy the redundancy condition around the α-methylene group. The bond charge parameters and the bond charge fluxes used for fatty acids are shown in Table 2.

Based on the bond polarizability model,[15—17] the Raman intensity parameters are composed of the equilibrium bond polarizabilities and their derivatives with respect to the internal coordinates. As in the case of the infrared intensity parameters, the equilibrium bond polarizability parameters and their derivatives concerning the stretching and the bending coordinates of the carboxyl group and those concerning the H–C_α and the C–C_α stretching coordinates were transferred from acetic acid.[3] The derived parameters for the bending coordinates of the α-methylene group were estimated by combining the values taken from the α-meth-

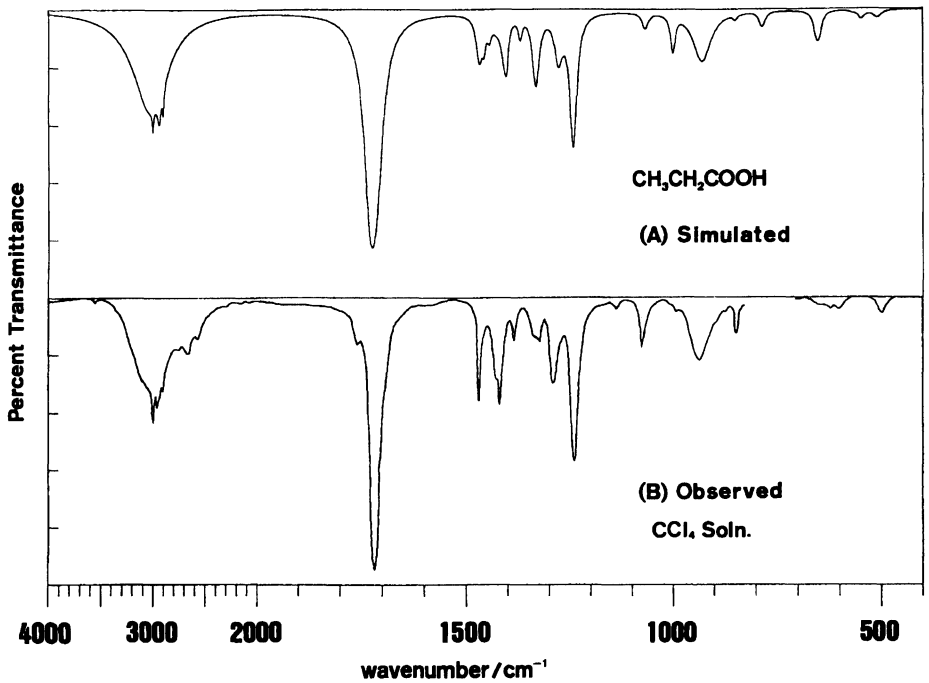

Fig. 6. Infrared spectra of propionic acid in CCl_4 solution at room temperature: (A) Simulated ($\omega_0=10$ cm^{-1}) and (B) Observed. The spectra was measured with a JASCO IRA-2 IR spectrometer: slit width 1.5 cm^{-1} at 1000 cm^{-1}; path length 0.1 mm. The concentration of propionic acid was 0.16 mol dm^{-3}.

yl group of acetic acid[3] with those of the methylene group of alkanes[28] and modifying them as required from the redundancy condition. The derived parameters $\partial\gamma^{L}_{C-O}/\partial\theta'_{HC_\alpha H}$ and $\partial\alpha^{E}_{C-O}/\partial\theta'_{HC_\alpha H}$ were indispensable for explaining the large Raman intensity of the $C_\alpha H_2$ bending mode of propionic acid dimer in the crystal. The Raman intensity parameters mentioned above are listed in Table 3.

Results and Discussion

The calculated geometries of the cis-conformer of propionic acid monomer and dimer are compared with the experimental values[22—24] and the calculated values by MM3[31] in Table 4. The calculated structures of propionic acid monomer and dimer agree well with the experimental data in the gas phase.[22,23] Our result of propionic acid monomer is comparable with the calculation by MM3[31] as a whole. The calculated structure parameters of butyric acid are compared with the experimental data in the crystal, determined by X-ray diffraction[25] in Table 5. The calculated hydrogen-bonded distances of propionic and butyric acids are closer to the data in the gas phase[22] than to those in the crystal,[24,25] since carboxylic acid in the simulation is isolated and the effect of compression in the crystal is not taken into account. The calculated hydrogen-bonded O···O distances of propionic and butyric acids in this work, 2.703 Å, can be made comparable with the observed ones in the crystal, 2.644 Å[24] (propionic acid) and 2.62 Å[25] (butyric acid), by considering the previously calculated compression effect [0.04—0.05 Å[32] and 0.070—0.089 Å,[33] (O···O distance in the isolated state) − (O···O distance in the crystal)]. The calculated dipole moment of propionic acid monomer, 1.56 Debye, is nearly equal to the observed value, 1.55 Debye ($D\approx 3.33564\times10^{-30}$C m).[23] The calculated dipole moment vector is tilted by 7.6° from the C=O bond toward the direction of the α-methylene group in the carboxyl plane. This value is in good agreement with the experimental value, 5°.[23] The calculated heats of formation of formic acid[1—3]through nonanoic acid are compared with the experimental values[26] and the results by MM3[31] in Table 6. The calculation in this work reproduces the observed values[26] within the range of experimental errors and is comparable with the MM3 values.[31]

The simulated and the observed infrared absorption spectra of crystalline propionic acid at 113 K and its deuterated species at liquid-nitrogen temperature are shown in Figs. 2, 3, 4, and 5. Previous investigations[18—21] of the infrared absorption spectra pointed out that propionic acid was exclusively in the cis-configuration below 120 K. Accordingly, only the spectra of the cis-configuration of propionic acid is used for the simulation. The half band widths of propionic acid at liquid-nitrogen temperature were assumed to be homogeneous. In Fig. 2, a part of the observed spectrum is compared with the simulated spectra of the cis- and the trans-conformers. The observed spectral pattern between 1500 and 1200 cm^{-1} is attributed more reasonably to the cis-conformer than to the trans-conformer. Particularly, the appearance of

the strong bands at 1332 and 1276 cm^{-1} in the simulated spectrum of the trans-conformer is not consistent with the observed spectrum. In Figs. 3, 4, and 5, the simulated infrared spectra of CH_3CH_2COOD, CH_3CD_2COOH, and CH_3CD_2COOD and the mixed spectra including possible isotopic impurities are compared with the observed spectra. The preference of the cis-conformer to the trans-conformer is clearly recognized for CH_3CH_2COOD in Figs. 3A, 3B, and 3D. The two strong bands near 1400 and 1250 cm^{-1} in the observed spectra are reproduced well by two bands at 1390 and 1246 cm^{-1} of the cis-conformer, but not by a single band at 1342 cm^{-1} of the trans-conformer. In Fig. 3C, the simulated spectra of CH_3CH_2COOD and CH_3CH_2COOH were superimposed at the ratio of 1:0.3 (CH_3CH_2COOD:CH_3CH_2COOH) to explain several bands marked with asterisk in the observed spectrum. The two bands between 950—900 cm^{-1} in the observed spectrum are apparently assigned to the doublet due to the Fermi resonance involving the OH out-of-plane bending mode of CH_3CH_2COOH.[20] In the cases of CH_3CD_2COOH (Fig. 4B) and CH_3CD_2COOD (Fig. 5B), possible isotopic impurities were used for superposition. The three bands (marked with asterisk) between 1250 and 1100 cm^{-1} in the observed spectra of CH_3CD_2COOH are accounted for by adding the spectra of $CH_3CHDCOOH$ and CH_3CH_2COOH (Figs. 4B and 4C). In Fig. 5, the spectra of $CH_3CHDCOOH$, CH_3CD_2COOH, and CH_3CH_2COOH were superimposed on that of CH_3CD_2COOD at the ratio of 1:0.1:0.1:0.05 (CH_3CD_2COOD : $CH_3CHDCOOH$: CH_3CD_2COOH: CH_3CH_2COOH), with the result that the bands marked with asterisk in the observed spectra were roughly simulated. On the whole, the overall features and the deuteration shifts are well reproduced in Figs. 2, 3, 4, and 5.

The simulated infrared absorption spectrum of a mixture of the cis- and the trans-conformers of propionic acid dimer is compared with the observed spectra at room temperature in the carbon tetrachloride solution in Fig. 6. According to the previous normal coordinate analysis by one of the authors,[20] the bands at 1290 and 1240 cm^{-1} in the observed spectra are assigned to the trans- and the cis-conformers, respectively. In order to simulate this splitting between the cis- and the trans-conformers, it was necessary to modify the values of the cross terms of the H–C_α–C bending and the C_α–C–O or the C_α–C=O bending coordinates transferred from acetic acid.[3] The cis-trans ratio in the simulation is so estimated to be 70:30, as to reproduce the spectral feature between 1300 and 1250 cm^{-1}. The ratio is consistent with the observed Raman spectra of liquid propionic acid, too. To reproduce the variation of the bandwidths observed in both the infrared absorption and the Raman spectra of fatty acids in the condensed phase, the half band width ω_a of the ath normal mode was calculated by Eq. 3,

$$\omega_a = \omega_0 \left(\sum_i \eta_i L_{ia}^2 / \sum_i L_{ia}^2 \right), \quad (3)$$

where ω_0 is the standard half band width, η_i is the half band width parameter[3] for the internal coordinate R_i, and L_{ia} is the i-a element of the $\boldsymbol{L}$matrix transforming the normal coordinates to the internal coordinates. The half band width parameters determined for acetic acid[3] in the carbon tetrachloride solution and in the liquid state were transferred to propionic acid in the solution (Table 7). As in the case of acetic acid, the infrared absorption intensities of propionic acid dissolved in carbon tetrachloride were corrected by multiplying the internal field factor, 1.30.[3,35] As a result, the overall tendency of the observed spectra are well simulated as shown in Fig. 6.

The observed Raman spectra of crystalline propionic acid at liquid-nitrogen temperature[20] is compared with the simulated spectra in Fig. 7. Judging from the simulated bands of the cis- and the trans-conformers between 1350 and 1200 cm^{-1}, it is obvious that the cis-conformer is predominant at liquid-nitrogen temperature, as in the cases of the simulated infrared absorption spectra of

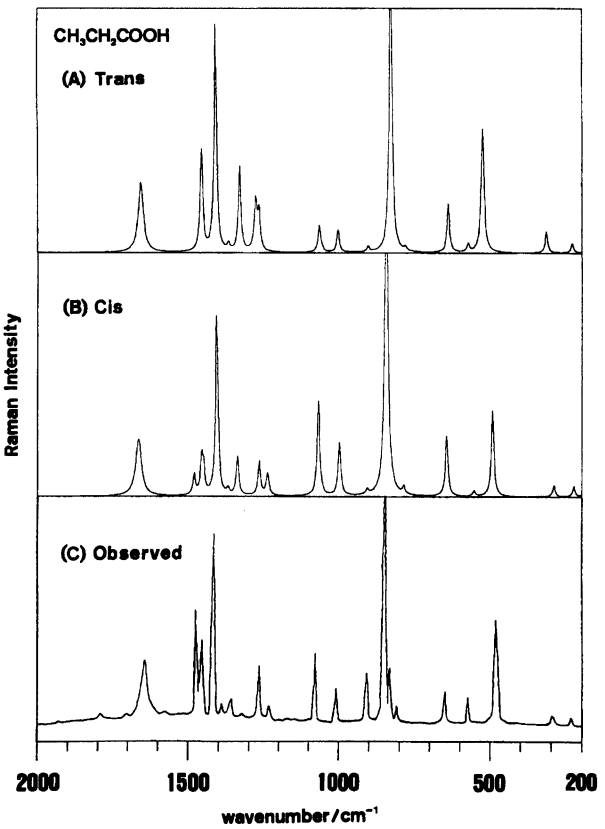

Fig. 7. Raman spectra of crystalline propionic acid at liquid-nitrogen temperature: (A) Simulated (ω_0=10 cm^{-1}); trans-configuration, (B) Simulated (ω_0=10 cm^{-1}); cis-configuration, (C) Observed, reproduced from *J. Mol. Struct.*, **36**, 35 (1977) (Ref. 20) with permission of Elsevier Science Publishers B. V.

crystalline propionic acid and its O-deuterated derivative (Figs. 2 and 3). The half band widths were assumed to be homogeneous except for the Raman active C=O stretching band. To simulate the observed band width near 1650 cm^{-1}, a new half band width parameter for the C=O stretching coordinate was introduced for the Raman spectra of fatty acids in the crystal.

The simulated and the observed Raman spectra of propionic acid at room temperature in the liquid state are compared with each other in Fig. 8. The spectra of the cis- and the trans-conformers were superimposed with the same ratio as used in Fig. 6. Concerning the Raman spectra of propionic acid in the liquid state, the half band width parameters for the C_α–C–O bending and the C_α–C=O bending coordinates were added to the parameters transferred from acetic acid[3] (Table 7). In the previous Raman spectral simulation of liquid acetic acid,[3] the half band width parameters for the C_α–C–O bending and the C_α–C=O bending coordinates were not necessary on account of the sharpness of the observed bands assignable to the O–C=O bending and the CO_2 rocking modes.[3] On the other hand, the considerable broadness of these bands in the observed spectra of liquid propionic acid (Fig. 8B) required the band width parameters for the related coordinates. In order to reproduce the broad width of the $C_\alpha H_2$ bending band in the observed spectrum, the Raman half band width parameter for the H–C_α–H bending coordinate of the α-methylene group of propionic acid was taken to be different from that of the $C_\alpha H_3$ group of acetic acid (Table 7). In the other respects, the simulated intensities and the band widths of propionic acid successfully reproduce the observed ones. According to the free energy difference between the cis- and the trans-conformers, the cis : trans ratio was calculated to be 90 : 10 at room temperature. The deviation of the calculated ratio from the observed ratio (cis : trans=70 : 30) may be attributed at least partly to the neglect of the intermolecular interaction in the condensed state.

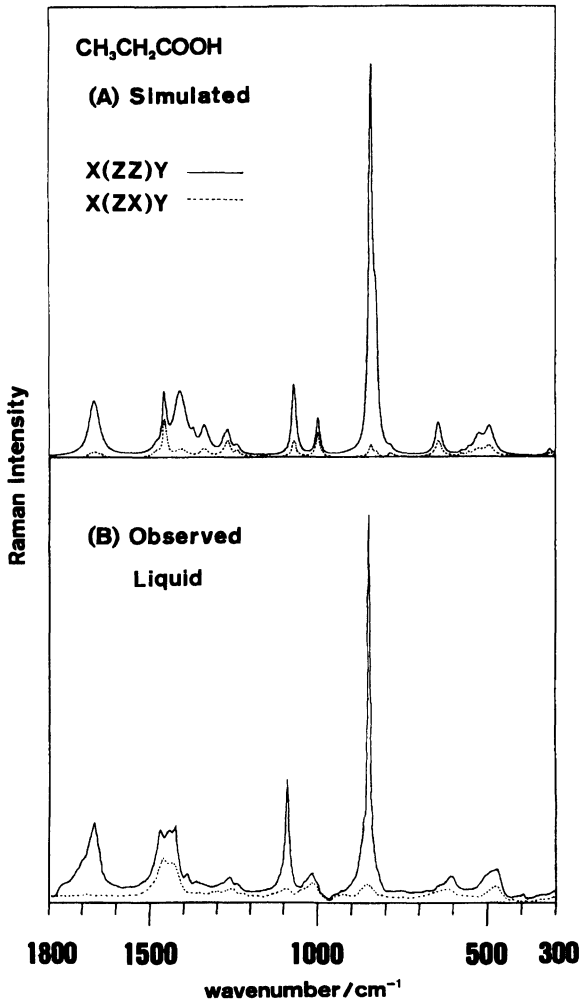

Fig. 8. Polarized Raman spectra of liquid propionic acid: (A) Simulated ($\omega_0 = 10$ cm^{-1}) and (B) Observed, recorded on a JEOL S-1 laser Raman spectrophotometer with a cooled HTV R649 photomultiplier, excited at 514.5 nm by a NEC GLG 3200 Ar^+ laser; slit width 6 cm^{-1} at 1000 cm^{-1}. The scattering geometry is X(Z,Z)Y (solid line) and X(Z,X)Y (dotted line).

The simulated and the observed infrared absorption spectra of crystalline lauric through palmitic acids at room temperature are shown in Fig. 9. At room temperature, the ratio of the cis-conformers to the trans-conformers in the even carbon-numbered fatty acids, belonging to the C-form crystal, was empirically estimated to be about 8 : 2.[19,21] A prominent feature of the cis-conformer is the multiple bands (below 1300 cm^{-1}) due to the CH_2 wagging modes coupled with the carboxyl vibrations.[21] On the other hand, the trans-conformer is characterized by the strong bands near 1300 cm^{-1}. For reproducing the multiple bands due to the CH_2 wagging modes, it was necessary to introduce the general valence-type cross terms of the C–O stretching coordinate with the $C_\alpha H_2$ wagging and the $C_\beta H_2$ wagging coordinates for the cis-conformer. The simulated spectra of the cis- and the trans-conformers of myristic acid are compared with each other in Fig. 10. The mixed spectra of the cis- and the trans-conformers at the above-mentioned ratio, 8 : 2, are shown in Fig. 9.

In the observed infrared absorption spectra of crystalline fatty acids at room temperature, the bands due to the OH stretching and the OH out-of-plane bending modes are far broader than the other bands (Fig. 9). Among the half band width parameters of acetic acid in the carbon tetrachloride solution and in the liquid state,[3] only those for the OH stretching and the OH out-of-plane bending coordinates were transferred to fatty acids in the crystal at room temperature. The calculated frequencies of the OH out-of-plane bending modes of lauric, myristic, and palmitic acids, 929, 930, and 930 cm^{-1}, are comparable with the observed values, 937, 938, and 940 cm^{-1} at room temperature, respectively, on transferring the OH out-of-plane bending force

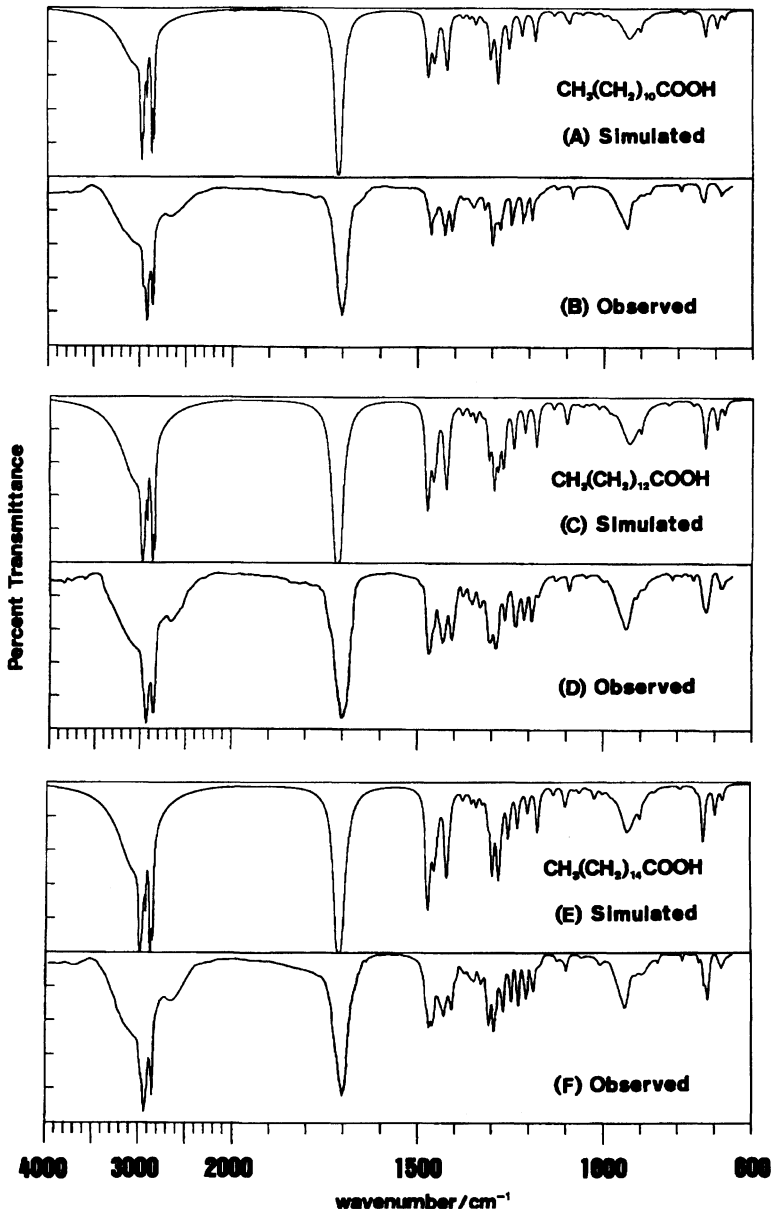

Fig. 9. Infrared spectra of crystalline fatty acid at room temperature. The observed spectra were reproduced from the IRDC cards with permission of Nankodo, Co., Ltd., Tokyo, Japan. Lauric acid: (A) Simulated ($\omega_0=10$ cm^{-1}) and (B) Observed (No. 134). Myristic acid: (C) Simulated ($\omega_0=10$ cm^{-1}) and (D) Observed (No. 168). Palmitic acid: (E) Simulated ($\omega_0=10$ cm^{-1}) and (F) Observed (No. 135).

constant from acetic acid[3] (0.1150 aJ rad^{-2}) to fatty acids. The broad band of the OH out-of-plane bending mode observed at room temperature is shifted upward by about 30 cm^{-1} on cooling to liquid-nitrogen temperature, and is split into sharp doublet bands at 963 and 976 cm^{-1} due to the cis- and the trans-conformers, respectively. To reproduce the upward shift and the cis-trans splitting, it was necessary to distinguish the OH out-of-plane bending force constants of the cis- and the trans-conformers from each other as shown in Table 1. The increase of the force constant from room temperature to liquid-nitrogen temperature may be ascribed to the intermolecular compression effect at low temperature. As a whole, the simulated spectra of lauric through palmitic acids are in good agreement with the observed spectra as shown in Fig. 9. The multiple bands due to the methylene wagging modes coupled with the C–O stretching mode are successfully reproduced.

The simulated Raman spectra of crystalline palmitic acid is compared with the observed spectra at room temperature in Fig. 11. As in the case of infrared absorption spectra of crystalline fatty acids at room temperature, the simulated spectra of the cis- and the trans-conformers were superimposed at the same ratio as in Fig. 9. In consequence of the simulation, the transfer of the Raman intensity parameters estimated for formic through propionic acids[1—3] to higher fatty acids is

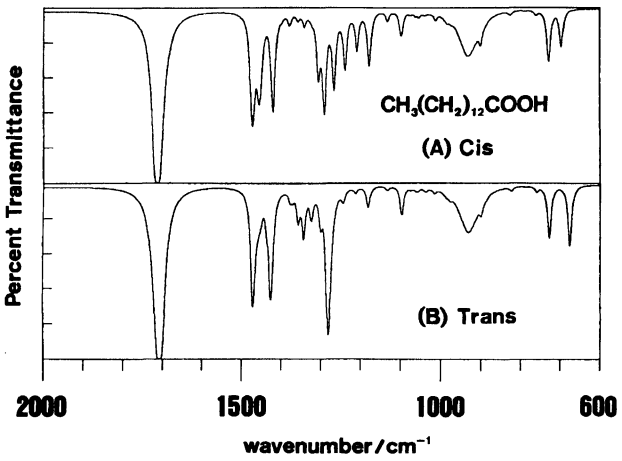

Fig. 10. Simulated infrared spectra of myristic acid dimer at room temperature ($\omega_0=10$ cm^{-1}). (A) cis-configuration and (B) trans-configuration.

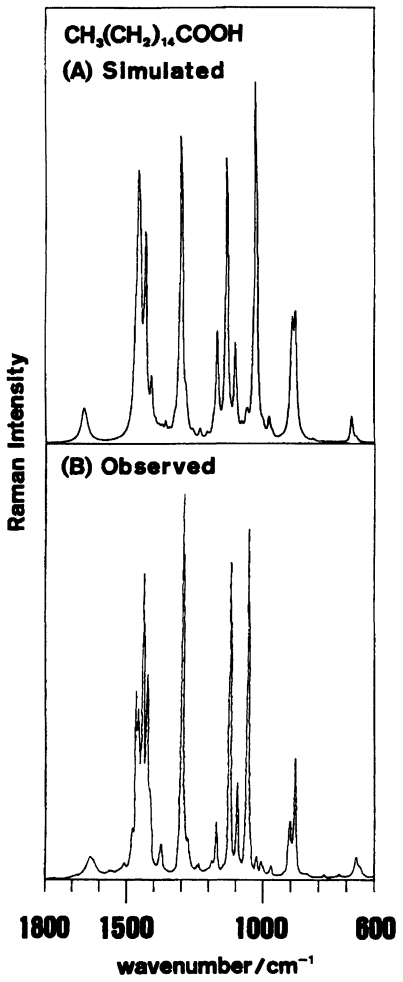

Fig. 11. Raman spectra of crystalline palmitic acid at room temperature: (A) Simulated ($\omega_0=10$ cm^{-1}) and (B) Observed, recorded on a JEOL JRS-U1 spectrophotometer with Ar^+ laser, excited at 488.0 nm; slit width 6.8 cm^{-1} at 1000 cm^{-1}. The scattering geometry is X(Z,X+Z)Y.

found to work very well. The half band width parameter for the C=O stretching coordinate, transferred from crystalline propionic acid, successfully reproduced the broad width of the band near 1650 cm^{-1} of higher fatty acid.

The enthalpy difference between the cis- and the trans-conformers of lauric acid was calculated to be 9.30 kJ mol^{-1}. This value deviates from the observed enthalpy difference ΔH (obsd)[19,21] of fatty acid belonging to the C-form crystal, -1.00 kJ mol^{-1} (decanoic acid) or -0.84 kJ mol^{-1} (tetradecanoic acid), by an amount ascribable to the effect of crystallization. Previously, the energy difference ΔH (total) ($=\Delta H$(trans)$-\Delta H$(cis)) was decomposed into the contribution from the intramolecular interaction ΔH (intra) and that from the intermolecular interaction ΔH (inter).[36] The latter was estimated to be -10.33 kJ mol^{-1} [36] (set 2, II) by considering the Coulomb interaction and the nonbonded interaction between the dimeric units. The values of ΔH (intra),[36] 7.41 kJ mol^{-1} (set 2) and 9.58 kJ mol^{-1} (set 5), are comparable with 9.30 kJ mol^{-1} in this work. The sum of ΔH (intra) in this work and ΔH (inter) in the previous work[36] is close to the negative values of the observed enthalpy difference, ΔH (obsd).[19,21]

The calculated and the observed frequencies of the

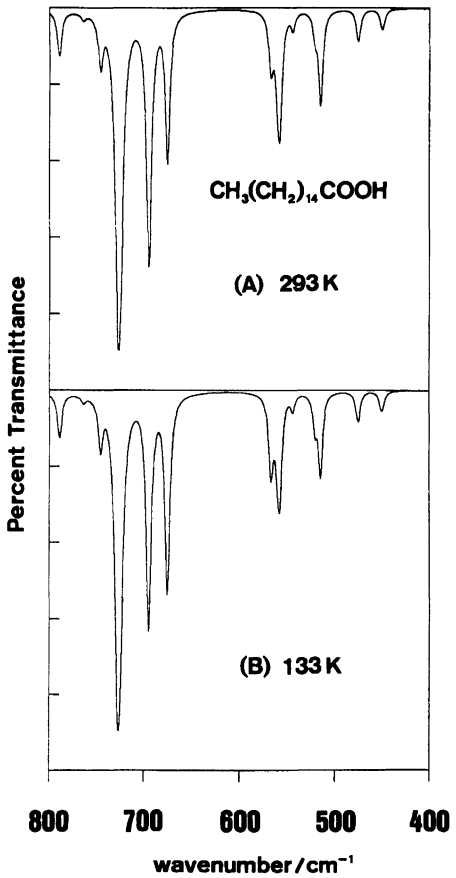

Fig. 12. Simulated infrared spectra of crystalline palmitic acid (A) at 293 K and (B) at 133 K ($\omega_0=5$ cm^{-1}).

O–C=O bending and the CO_2 rocking modes of propionic through palmitic acids are listed in Table 8. In the cases of longer fatty acids belonging to the C-form crystal, modification of the relevant force constants of propionic acid dimer belonging to the C′-form crystal (Table 1) was found necessary for simulating the observed frequencies of the O–C=O bending and the CO_2 rocking modes of them. The simulated infrared absorption specra of crystalline palmitic acid between 800 and 400 cm^{-1} at 293 and 133 K are illustrated in Fig. 12. The cis : trans ratios in the simulation at 293 and 133 K were taken from the experimental ratios, 8 : 2 and 7 : 3,[19,21] respectively. The simulated spectra follow well the temperature-dependent intensity variations observed for the O–C=O bending modes of the cis- and the trans-conformers.[37]

In conclusion, the potential and the intensity parameters transferred from acetic acid and alkanes in the gas phase were found to be effective for reproducing the thermodynamic quantities, the structures, the vibrational spectra of fatty acids. Particularly, accurate description of the charge distribution around the carboxyl group and the α-methylene group (Tables 2 and 9) based on the gas-phase data[1,3] successfully elucidates the infrared absorption spectra of propionic acid and longer fatty acids in the crystal (Figs. 2, 3, 4, 5, 9, 10, and 12) and in the carbon tetrachloride solution (Fig. 6).

The numerical calculations were carried out on FACOM M-1800 computer system at the Data Processing Center of Kyoto University.

References

1) I. Yokoyama, Y. Miwa, and K. Machida, *J. Am. Chem. Soc.*, **113**, 6458 (1991).
2) I. Yokoyama, Y. Miwa, and K. Machida, *J. Phys. Chem.*, **95**, 9740 (1991).
3) I. Yokoyama, Y. Miwa, and K. Machida, *Bull. Chem. Soc. Jpn.*, **65**, 746 (1992).
4) J. C. Decius, *J. Mol. Spectrosc.*, **57**, 348 (1975).
5) Y. Maréchal, *J. Chem. Phys.*, **87**, 6344 (1987).
6) Y. Maréchal, "Vibrational Spectra and Structure," ed by J. Durig, Elsevier, Amsterdam (1987), Vol. 16, Chap. 5, pp. 311—356.
7) a) D. Berckmans, H. P. Figeys, and P. Geerlings, *J. Phys. Chem.*, **92**, 61 (1988); b) D. Berckmans, H. P. Figeys, Y. Maréchal, and P. Geerlings, *J. Phys. Chem.*, **92**, 66 (1988).
8) J. E. Bertie and K. H. Michaelian, *J. Chem. Phys.*, **76**, 886 (1982).
9) J. E. Bertie, K. H. Michaelian, H. H. Eysel, and D. Hager, *J. Chem. Phys.*, **85**, 4779 (1986).
10) R. C. Millikan and K. S. Pitzer, *J. Am. Chem. Soc.*, **80**, 3515 (1958).
11) a) M. Haurie and A. Novak, *J. Chim. Phys.*, **62**, 137 (1965); b) M. Haurie and A. Novak, *J. Chim. Phys.*, **62**, 146 (1965).
12) J. L. Derrisen, *J. Mol. Struct.*, **7**, 67 (1971).
13) M. D. Harmony, V. W. Laurie, R. L. Kuczkowski, R. H. Schwendeman, D. A. Ramsay, F. J. Lovas, W. J. Lafferty, and A. G. Maki, *J. Phys. Chem. Ref. Data*, **8**, 619 (1979).
14) B. P. van Eijck, J. van Opheusden, M. M. M. van Schaik, and E. van Zoeren, *J. Mol. Spectrosc.*, **86**, 465 (1981).
15) M. Gussoni, S. Abbate, and G. Zerbi, *J. Raman Spectrosc.*, **6**, 289 (1977).
16) S. Abbate, M. Gussoni, and G. Zerbi, *Indian J. Pure Appl. Phys.*, **16**, 199 (1978).
17) M. Gussoni, "Vibrational Intensities in Infrared and Raman Spectroscopy," ed by W. B. Person and G. Zerbi, Elsevier, Amsterdam (1982), Chap. 11, pp. 221—238.
18) S. Hayashi, H. Hara, and N. Ķimura, *Bull. Inst. Chem. Res., Kyoto Univ.*, **46**, 213 (1968).
19) S. Hayashi and J. Umemura, *J. Chem. Phys.*, **63**, 1732 (1975).
20) J. Umemura, *J. Mol. Struct.*, **36**, 35 (1977).
21) J. Umemura, *J. Chem. Phys.*, **68**, 42 (1978).
22) J. L. Derissen, *J. Mol. Struct.*, **7**, 81 (1971).
23) a) O. L. Stiefvater, *J. Chem. Phys.*, **62**, 233 (1975); b) O. L. Stiefvater, *J. Chem. Phys.*, **62**, 244 (1975).
24) F. J. Strieter, D. H. Templeton, R. F. Scheuerman, and R. L. Sass, *Acta Crystallogr.*, **15**, 1233 (1962).
25) F. J. Strieter and D. H. Templeton, *Acta Crystallogr.*, **15**, 1240 (1962).
26) J. B. Pedley, R. D. Naylor, and S. P. Kirby, "Thermochemical Data of Organic Compounds," 2nd ed, Chapman and Hall, London (1986).
27) K. Machida, H. Noma, and Y. Miwa, *Indian J. Pure Appl. Phys.*, **26**, 197 (1988).
28) Y. Miwa and K. Machida, *J. Am. Chem. Soc.*, **110**, 5183 (1988).
29) W. T. King, G. B. Mast, and P. P. Blanchette, *J. Chem. Phys.*, **56**, 4440 (1972).
30) L. Pauling, "The Nature of the Chemical Bond," Cornell University, Ithaca, New York (1960).
31) N. L. Allinger, Z. S. Zhu, and K. Chem, *J. Am. Chem. Soc.*, **114**, 6120 (1992).
32) R. Nakamura, K. Machida, M. Oobatake, and S. Hayashi, *Mol. Phys.*, **64**, 215 (1988).
33) S. Hayashi, M. Oobatake, R. Nakamura, and K. Machida, *J. Chem. Phys.*, **94**, 4446 (1991).
34) D. R. Stull, E. F. Westrum, Jr., and G. C. Sinke, "The Chemical Thermodynamics of Organic Compounds," Wiley, New York (1969).
35) S. R. Polo and M. K. Wilson, *J. Chem. Phys.*, **23**, 2376 (1955).
36) S. Hayashi, J. Umemura, and R. Nakamura, *J. Mol. Struct.*, **69**, 123 (1980).
37) G. Zerbi, G. Minoni, and A. P. Tulloch, *J. Chem. Phys.*, **78**, 5853 (1983).